Journal of Current Science and Technology, January-April 2024 Vol. 14 No. 1, Article 12

ISSN 2630-0656 (Online)

Cite this article: Hariharan, S., Marimuthu, U., Sundaresan, T., Shanmugam, S. K., Radhakrishnan, R. G., Mierzwinshi, D., & Walter, J. (2023). Wire electric discharge machining of aluminium hybrid composite: renewable energy based IoT approach. *Journal of Current Science and Technology*, *14*(1), Article 12. https://doi.org/10.59796/jcst.V14N1.2024.12

Journal of Current Science and Technology

Journal homepage: https://jcst.rsu.ac.th

Wire Electric Discharge Machining of Aluminium Hybrid Composite: Renewable Energy Based IoT Approach

Sreeram Hariharan[1], Uthayakumar Marimuthu[1*], Thirumalaikumaran Sundaresan[2], Suresh Kumar Shanmugam[1], Rajeshkanna Govindhan Radhakrishnan[3], Darius Mierzwinshi[4] and Janusz Walter[4]

[1]Department of Mechanical Engineering, Kalasalingam Academy of Research & Education, Krishnan Koil 626126, Tamil Nadu, India
[2]Department of Mechanical Engineering, PSG Institute of Technology and Applied Research, Coimbatore 641062, Tamil Nadu, India
[3]Department of Electrical and Electronics Engineering, Kalasalingam Academy of Research & Education, Krishnan Koil 626126, Tamil Nadu, India
[4]Faculty Material Engineering and Physics, Cracow University of Technology, 30010, Poland

*Corresponding author; E-mail: uthaykumar@gmail.com

Received 9 June, 2023; Revised 23 September, 2023; Accepted 6 October, 2023
Published online 6 December, 2023

Abstract

Wire Electric Discharge Machining (WEDM) has been recognized as one of the optimum methods for machining of harder aluminum-based hybrid metal matrix composites (AHMMC). This method is used to optimize the major control aspects of a machine and they are current, pulse duration, and rate of feed of wire on kerf width (KRW) and Surface roughness (Ra) of hybrid composites made of aluminum Al6351 as the metal matrix (AMMHC). The AMMHC has been created via a stir casting technique by adding SiC and B_4C with an Al6351 matrix. Box-Behnken design (BBD) has been used to conduct tests in order to parametrically optimize the WEDM process. The optimization of KRW and Ra is identified using 3-D surface plots, graphs and response table of ANOVA as well as by employing Response Surface Methodology (RSM). Internet of Things (IoT) is implemented to monitor the quality of electrolyte that is used in WEDM. It has been identified that the current has a major contribution in both KRW and Ra factors. A lower current is preferred for a lower KRW whereas higher current improves R_a value.

Keywords**:** *Wire electric discharge machining; Internet of Things; Hybrid composite; Renewable energy*

1. Introduction

Due to the rapid developments in the mechanical industry, the requirement of composite materials with higher durability and extreme hardness has increased in the recent past (Gautam et al, 2022; Gu, 2023; Zhang, 2022). By using the conventional machining techniques, machining of such materials is challenging to handle. Hence, the unconventional techniques for machining like electrical discharge machining, electrochemical machining, ultrasonic machining, are implemented for facing such challenging materials (Cui et al, 2022; Hynes et al, 2022; Khazaal et al, 2022). Regardless of the hardness, Wire Electric Discharge Machining (WEDM) is a widely accepted non-conventional material removal technique that is used to create objects with complex forms and profiles (Singh et al, 2022; Tan et al, 2022; Wang, 2023). WEDM is a high accuracy machine and it is most widely used to create apparatuses, instrument, shape etc. WEDM is equipped to perform accurate machining that has left away surprising forms or perplexing shapes which are challenging to manufacture using conventional machining

techniques. In WEDM machining, material removal is achieved by producing spark between the wire cathode & the work piece which is connected as the anode. The WEDM has become a simple process for constructing instruments and it is now the finest choice for creating miniature sizes, and for providing the highest level of dimensional accuracy as well as surface finish. The present-day industry calls for improved productivity with improved machining characteristics for the sustainability and for which, WEDM can be identified as one of the best options. Mechanical characteristics such as creep life, conductivity, obstruction to erosion, and so on, depend on the sur-face quality of the machined workpiece. (Liang et al, 2020; Xie et al, 2021; Yan et al, 2022; Zhu, 2022) Nevertheless, a variety of factors in-fluences the WEDM machining cycle, due to the interaction of stochastic character and multiple barriers.

The goal of response surface methodology (RSM), a collection of real and quantitative techniques, is to streamline the process by examining and exhibiting the issue in which a reaction to be of interest is affected by a number of different parameters (Boutrih et al, 2022; Erol et al, 2022; Kumar et al, 2022; Sudhakar et al, 2022). The type of link between the free components and their influence on the output parameters is ambiguous in majority of RSM problems. Finding a fair assessment of the unaltered functional link between the output response "y" and the provision of free components is the initial step in RSM (Govindarajulu, 2021; Paulson et al, 2022; Roy et al, 2022; Tata et al, 2021). A minimal polynomial with least gap between the independent variables is typically used for the evaluation of the output parameters. If direct capability of the unrestricted variables is used to represent the reaction all around, then the approximation capacity is the main request model. A higher-order polynomial, such as the second-order model is used, if the response system is curved. (Badizi et al, 2020; Calam et al, 2022; Velavan et al, 2023). Golshan et al. (2012). have conducted the evaluation of Al-SiC composites using genetic algorithm for generating the ideal MRR and R_a of the composite. Since both the analyzing parameters are in contrast, the manuscript has chosen multi-response algorithm to optimize both the parameters. Single Genetic Algorithm (SGA) and non-dominated sorting genetic algorithm (NSGA-II) are employed for the optimization and the work is finalized based on the NSGA-II algorithm. The optimization of the current, pulse duration, gap voltage and the volume fraction of SiC of the composite was targeted by the work. The work has identified that the optimization in both targeted variables can be achieved by variation in the voltage as well as the volume fraction of SiC. The algorithm was capable of predicting the targeted parameters for the design parameters. Jithin, & Suhas (2021) conducted a comprehensive analysis of modified EDM and an Electric Discharge Texturing (EDT) is used for different applications. The review has evaluated various levels of EDT applications and versions of EDT employed for different uses. The paper has analyzed different parameters which influence the topology of the surface in EDT. The work also analyzed the change in surface roughness due to the variation in the control parameters. The work also covered the evolutions of purposeful surface alterations made with EDM and EDT. In this paper, various modelling approaches are examined alongside a comparison of output models. The research has shown that a 3D multi-crater analysis is necessary for an accurate modelling of EDT. Peta et al. (2021a) have evaluated the surface topology due to the EDM machining of AA6060 alloy based on discharge energy. According to the study, discharge energy has a significant impact on surface topology, and the EDM machine controls the parameters related to discharge energy. Below 11μm, the model was unable to provide satisfactory results. It was evident that the values ranging from 36μm to 41μm have produced the greatest results in terms of the link between surface topology and discharge energy. Peta et al. (2021b) have conducted experimental analysis to ascertain the connection of the wettability with the microgeometry of the surface of AA6060 alloy. The work discovered a strong link between the parameters related to surface topology and the wettability of the sample. The discharge energy and the contact angle, which is the inverse of the material's wettability, are found to have a direct relationship with the size and shape of the surface produced by EDM. Joshi et al. (2011) have conducted experimental analysis on the stainless-steel surfaces machined by EDM in a field of magnetic pulsation using copper electrode. It was identified that the additional magnetic field improved the spark density. The experimental study identified a 130% improvement in MRR with no electrode wear. The improvement of pool boiling

heat transfer of Al6061 alloy through EDM has been studied by Dhadda et al. (2021). Discharge current and pulse-on-time are the input parameters that were taken into account for the investigation. The association between the surface topology and the boiling performance during the machining process has been determined using a data-dependent system. The crater diameter is shown to be more correlated with the average roughness parameter. Al7075 alloy, which has been widely utilized in the aerospace sector, was the subject of a study by Golshan et al. (2013). The dimensions inaccuracy and surface roughness of the drilled hole are optimized using the NSGA-II algorithm. Cutting speed, feed rate, and drill diameter are regarded as the model's most crucial input parameters. The relationships between the dimensional inaccuracy and surface roughness are observed to follow a linear pattern. The program can determine the dimensional inaccuracy for the desired surface roughness or vice versa. In order to simulate drilling in CFRP laminates, Saravanan et al. (2012) used numerical and finite element analysis (FEA), and the outcomes were compared to those obtained by experimentation. The genetic algorithm was employed for numerical analysis, revealing a 10% variation in the evolutionary algorithm-based mathematical model and a 20% variation in the FEA evaluation. The optimal input parameter conditions for better output parameters have also been determined by the numerical analysis. An extensive study on the reinforcement using Al_2O_3 was carried out by Khajuria et al (2018, 2019) for the machinability and optimization of the AA2014 Aluminum Alloy. The experiments were carried out by machining the composite in Die sinking EDM. Akhtar, & Khajuria (2023) carried out the detailed study of the grain structure and the metrological properties due to the different conditions. The normalized and tempered condition properties were evaluated and the modifications occurring in the grain boundaries were studied in the work. The experimental results were compared with the simulated model.

The effects of three WEDM input process factors, namely pulse current, pulse duration period, and speed of a wire drum on the output parameters of surface roughness and kerf width have been evaluated through the machining of hybrid composite. These procedure parameters ranges are determined using the results of the previous experimental studies. Box- Behnken design (BBD) has been identified as a quicker and relatively accurate method that can be used for the optimization of process parameters and hence, this method has been more frequently used by researchers than that of the central composite design. Table 1 presents the values of distinct metrics and Table 2 provides the details of the output parameters obtained for 15 experiments carried out for the experimental evaluation. The IoT based system has been implemented to monitor the flow of electrolyte to ensure a uniform flow throughout the experimental study.

2. Objectives

To propose a method for optimizing the major control aspects of wire electric discharge machining of Aluminium hybrid.

3. Materials and methods

The stir casting process has been employed in this work to manufacture hybrid metal matrix components. In Al6351 matrix, 5 wt% SiC and 3wt% B_4C are added to manufacture the hybrid composite. The details of the process used for stir casting is as follows:

The casting die was initially preheated to 400°C. Al6351 rod with length of around 25 mm was added into the crucible. The crucible was kept in the furnace. The alloy was heated to the temperature of 850°C inside the crucible for taking it above the liquidous state. The molten metal is stirred using a stirrer at 700 rpm and allowed to cool down slowly. The reinforcement is slowly added to the molten metal without stopping the stirring action. 2% Magnesium is added to the molten composite to improve its wettability. The molten mixture is poured into the preheated rectangular die of size 200 mm x 150 mm x 30 mm to obtain the final composite.

RSM's three factors, 3-level Box-Behnken design has been employed in the experiment approach (BBD). The BBD is especially good in the second order model's fitting in RSM with the least amount of analysis. In this investigation, a BBD design comprising three parameters and 15 runs has been used. By utilizing the data from 15 tests, the experiment has been created. For the machining of Al6351- SiC-B_4C, three independent variables are identified based on the previous works. A Wire EDM machine is employed for the experiment. Figure 1a demonstrates the WEDM test setup. In this experiment, deionized liquid serves as the

cooling medium while brass wire of 0.25mm diameter serves as the cutting tool. Surft-est-SJ201 has been utilized to measure the surface roughness of all the specimens with the measuring range of 350µm (-200µm to +150µm) with a measuring speed of 0.25mm/s. The traverse length of all the specimen is fixed as 1.25mm on the machined surface of the fabricated object. Fig 1.b provides the specimen developed using stir casting method. Figure 2 shows the sample graph of the measurement details of the surface roughness that is measured using the instrument. The tool makers' microscope is used for measuring the kerf width and the statistical analysis is per-formed using Minitab software. In the machining process, the quality of the electrolyte is to be maintained and hence, IoT based sensors are used to detect the purity of the electrolyte. The turbidity sensor is connected in the electrolyte tank and it is connected with the arduino Uno board. The connections are given as shown in figure 3. If the quality of the electrolyte decreases, then the intimation will be given through the arduino. The power required to operate the IoT will be drawn from the solar renewable energy. Figure 3b shows the turbidity sensor connected with the electrolyte tank. Figure 3c shows the turbidity sensor connected with the arduino uno board and the alert sys-tem. Figure 3d shows the connection diagram of the Internet of Things.

The basic instruments and machines used for the experimental investigation are provided in Table 1.

The measurement of Kerf width was carried out using the specified device in Table 1 having 100× magnification level. The surface roughness instrument was having a testing accuracy of 1 micron. Totally, 15 tests are carried out by changing the set of parameters as shown in Table 2.

The details of the input and the output values of the experiment are provided in Table 3 along with the analysis data compiled using BBD.

Table 1 Instruments and machines employed

Model	Wire EDM (Model:DK7750, M/s Concord United Products Private Limited, Bangalore, India)
Tool	Brass wire (0.25 mm diameter)
Dielectric fluid	Deionized water
Flushing flow rate	9 l/min
Surface roughness measuring device	Mitutoyo, Model: Surf test SJ-201 (Mitutoyo, Kanagawa, Japan)
Kerf width measuring device	Tool-makers' microscope

Table 2 Various Parameters with different operating levels.

Parameters	**Operating levels**		
	-1	**0**	**1**
Current	12A	16A	20A
Pulse duration (Ton) (µm)	100 µm	110 µm	120 µm
Rate of feed of wire (WFR)	6 m/min	8 m/min	10 m/min

Figure 1a Wire EDM machine Set-up

Figure 1b Composite specimen for wire EDM machining

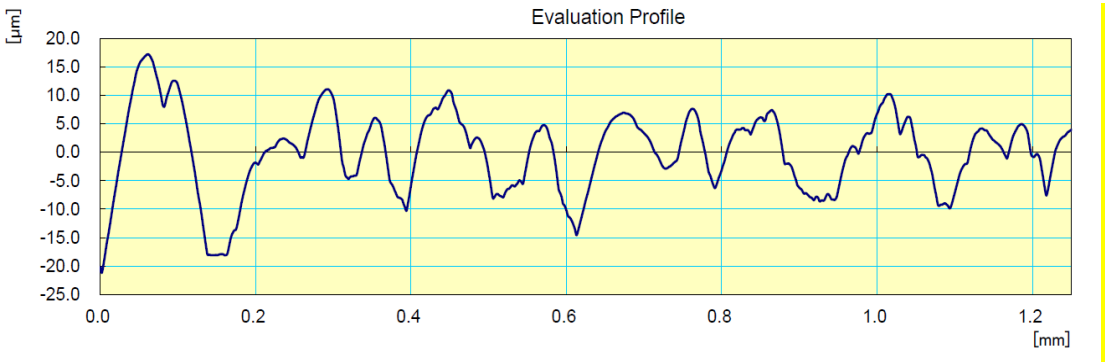

Figure 2 Sample surface roughness measurement graph plotted using SJ201

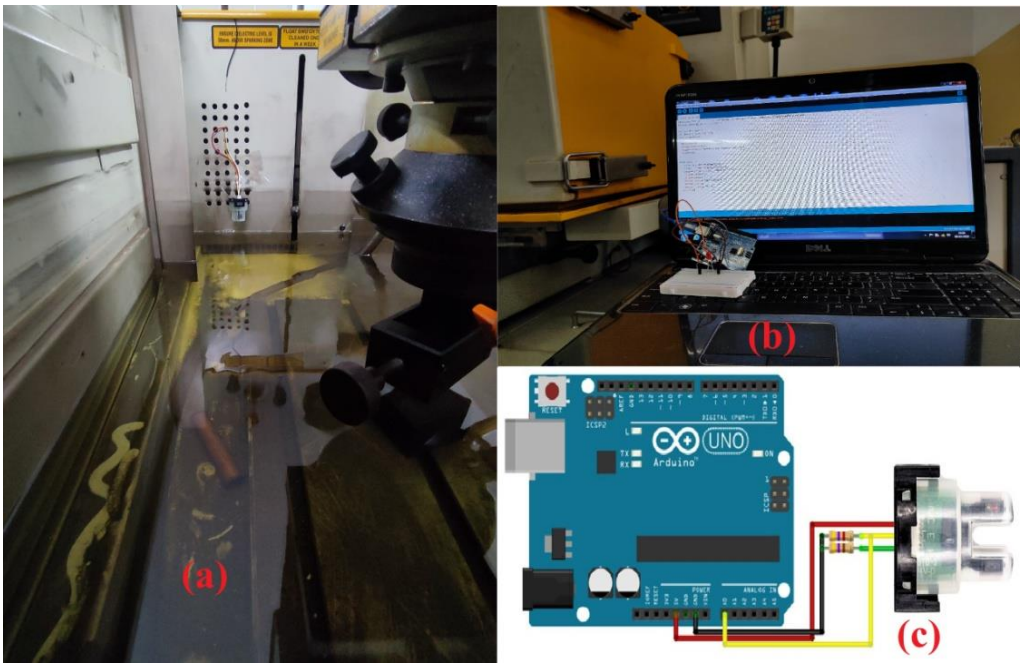

Figure 3a Turbidity sensor connected in electrolyte tank, **3b** Arduino Uno Connection with sensors and alert system, **3c** Connection diagram of IoT

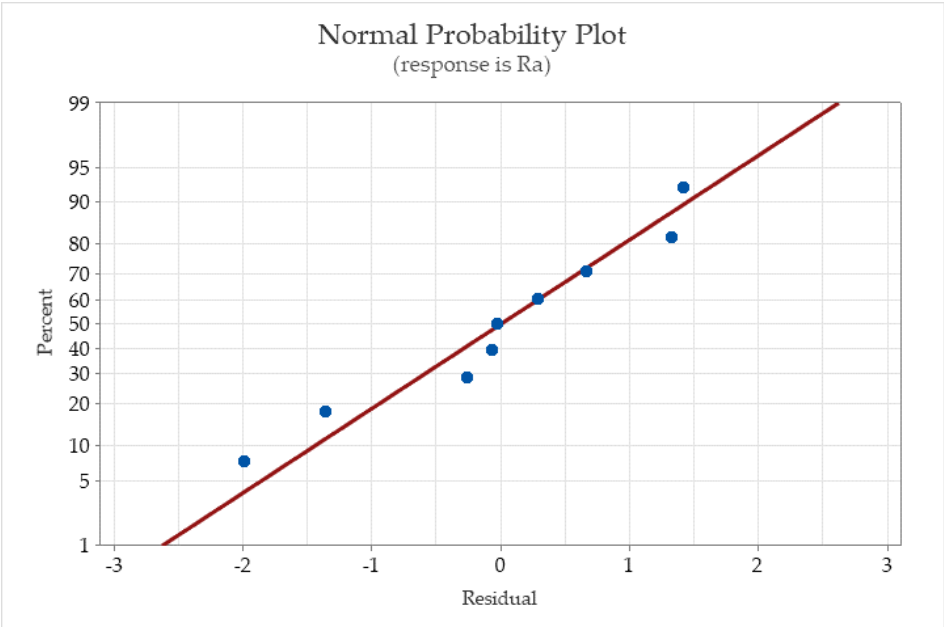

Figure 4 Typical probability plot - Surface roughness: Experimental Vs Expected

Table 3 Experimental data with the analyzed data providing the Standard Order.

Std Order	Run Order	Pt Type	Blocks	Current (A)	Pulse duration (T_{on})	Rate of feed of wire (WFR)	Kerf width (KRW)	Surface roughness (Ra)
9	1	2	1	16	100	6	0.23	5.12
14	2	0	1	16	110	8	0.21	10.68
13	3	0	1	16	110	8	0.21	10.68
10	4	2	1	16	120	6	0.22	6.79
8	5	2	1	20	100	10	0.36	11.98
4	6	2	1	20	120	8	0.38	3.94
11	7	2	1	16	100	10	0.23	5.12
7	8	2	1	12	110	10	0.21	8.63
6	9	2	1	16	110	6	0.22	6.79
2	10	2	1	20	100	8	0.39	5.241
15	11	0	1	16	110	8	0.21	6.79
12	12	2	1	16	120	10	0.23	8.56
1	13	2	1	12	100	8	0.09	7.79
3	14	2	1	12	120	8	0.1	7.646
5	15	2	1	12	110	6	0.12	5.08

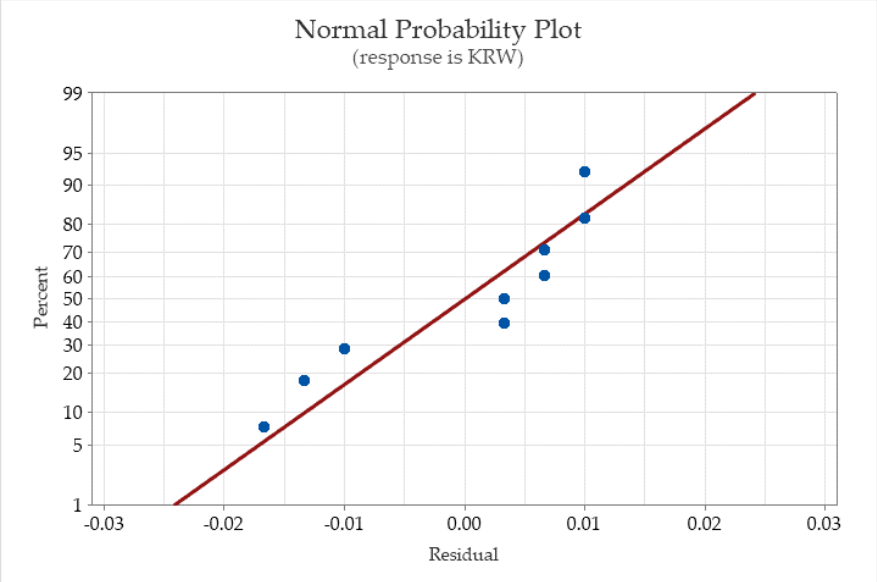

Figure 5 Normal probability plot- Kerf width: Experimental Vs Predicted

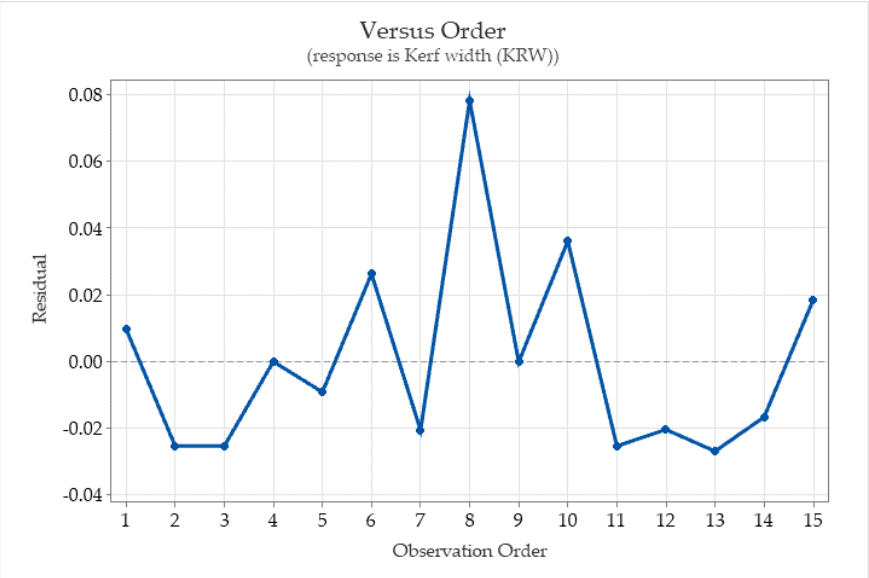

Figure 6 Kerf width response order

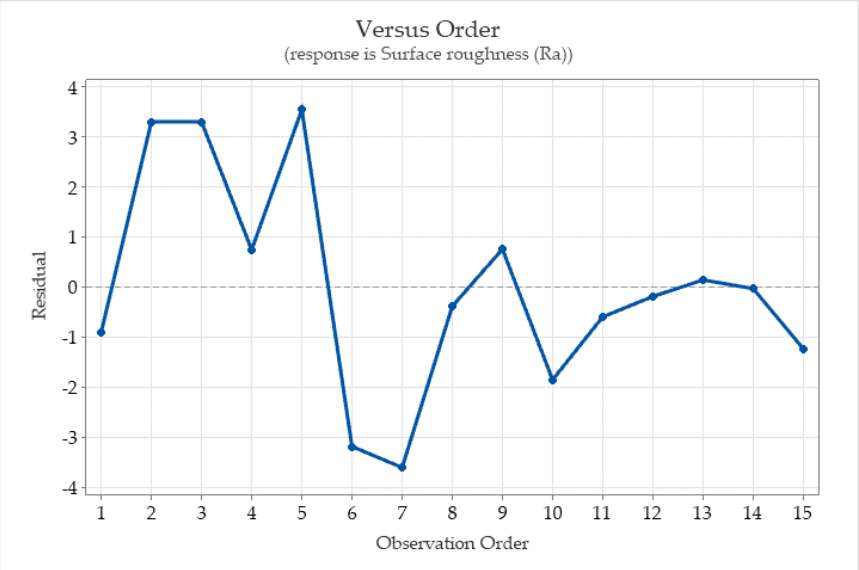

Figure 7 Surface roughness response order.

4. Results

To establish how the control parameters affect the surface finish, surface plots are used, based on the major input parameters, as demonstrated in figures. 8-13. Based on the normal probability curve displayed in figure 4, a more accurate experimental measurement is recorded during the test. A similar pattern is observed for KRW as displayed in figure 5. The primary parameter for the variation of Ra has been identified as current. A spark's magnitude crater, such as shallow ones that offer better Ra, is linked with the spark energy.

The figures 4 and 5 show normal probability plots which indicate the variation of the experimental result from the predicted result based on the mathematical formulation. It clearly indicates that the mathematical formulation is closely matching with the experimental results. Therefore, the model developed can be considered for further evaluation of the machining process and the parameters considered are the major contributors for the machining output parameters

considered and they are surface roughness and kerf width. Figures 6 and 7 show the response plot to identify the independence of the considered input variables and they are employed for investigating the output parameters. The response plot zig zag pattern clearly shows that the input parameters considered do not show any dependency on each other for the output parameters. Therefore, the parameters considered for the evaluation are completely independent variables

Figure 8 shows the surface plot of surface roughness by considering current and pulse duration. It can be clearly seen that higher and lower pulse duration produce a lower surface roughness even at higher current condition, but a lower current at higher pulse duration increases the surface roughness. This can be attributed to the condition that the increased spark energy can improve the surface finish. At the medium pulse duration, there is an increase in surface roughness, due to the improper removal of material, especially at the lower current zone. Figure 9 provides the surface plot for the kerf width with respect to current and pulse duration. The kerf width is low at the lower current range, since higher current provides higher energy for removing more materials than the size of the wire. At lower current, therefore, kerf width is lower, which is preferred for high precision machining. Figure 10 shows the surface plot with the input parameters, current and rate of feed of wire for evaluating the variation in the surface roughness. It can be identified that higher current and a lower rate of feed of wire provide a lower surface roughness. The lower rate of feed of wire helps for a proper material removal by improving the surface finish compared to higher feed rate. In figure.11, the variation of kerf width based on current and rate of feed of wire is examined using the surface plot. It can be identified that the lower current and higher rate of feed of wire reduce the kerf width. The higher rate of feed of wire distributes the spark properly on the surface by reducing the kerf width. Figure 12 provides the surface plot of the surface roughness based on the pulse duration and the rate of feed of wire. A lower pulse duration and a lower rate of feed of wire provides a lower surface roughness. The rate of feed of wire has more contribution to the surface roughness compared to the pulse duration and it can be clearly seen in the graph. Figure 13 provides the surface plot of the kerf width for the input parameters of pulse duration and rate of feed of wire. It can be clearly seen that these parameters have no influence of kerf width on these two parameters, as the kerf width is constant for the variations of these two parameters. Therefore, it can be understood that current has a greater influence on the kerf width compared to other two parameters.

If these graphs are considered, the following points can be identified

• The increased pulse duration increases the surface roughness which can be identified from the surface plots in figures 8 and 12. Therefore, a lower pulse-on-time is preferred for better surface roughness of the composite material.

• From figures 10 and 12, surface roughness is seen to increase with an increase in rate of feed of wire. The reduced rate of feed of wire improves the surface roughness, as the material removal from a specific zone will be better at a lower rate of feed of wire.

• At a lower wire feed and pulse-on time, the higher current does not create too much variations in the Ra and it can be clearly observed in figures 8 and 10. But, if the feed rate is increased, a lower current can provide pulse-on-time and a lower current can provide a better surface finish.

When these parameters are considered for variation in kerf width, the surface plots of them are provided in figures 9,11 and 13. It can be clearly seen from the graphs in figures 8 and 10 that the increase in the current increases the kerf width. Figure 13 indicates that the kerf width has no implications on the variations of wire feed and the pulse-on -time, as the variation in kerf width is identified to be negligible throughout the range of graph. From the graphs of current, a medium level pulse-on-time and a higher rate of feed of wire reduce the kerf width. The lower kerf width can be obtained by lower current, medium level pulse-on-time and high wire feed.

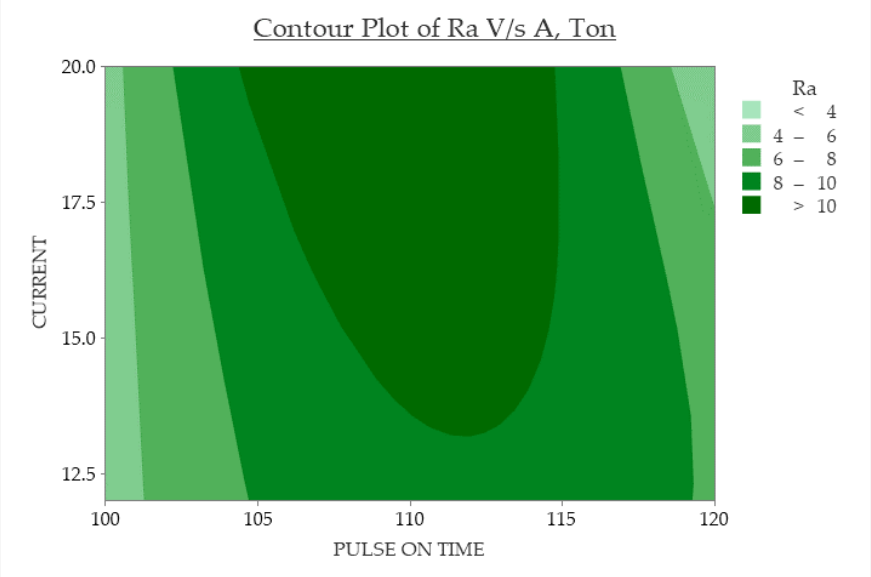

Figure 8 Contour surface plot: Surface roughness with Current & pulse duration

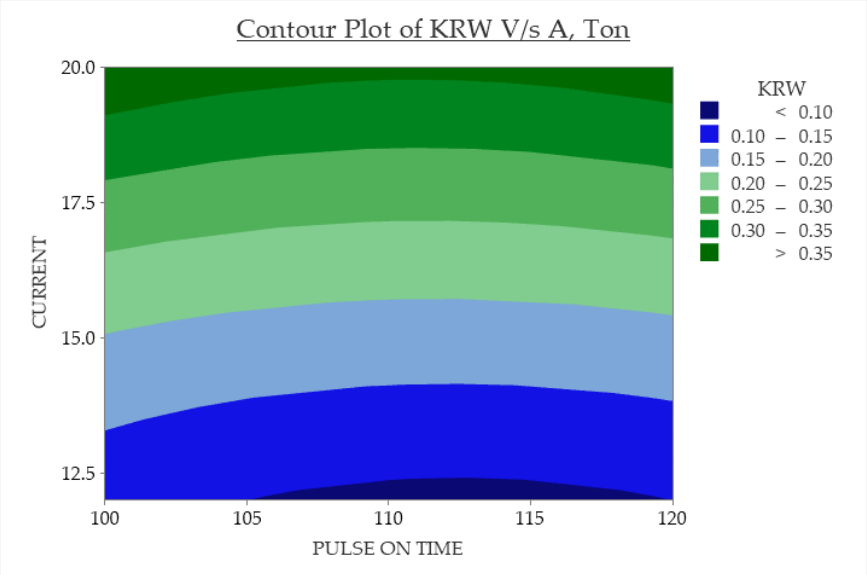

Figure 9 Contour surface plot: Kerf width with Current & pulse duration

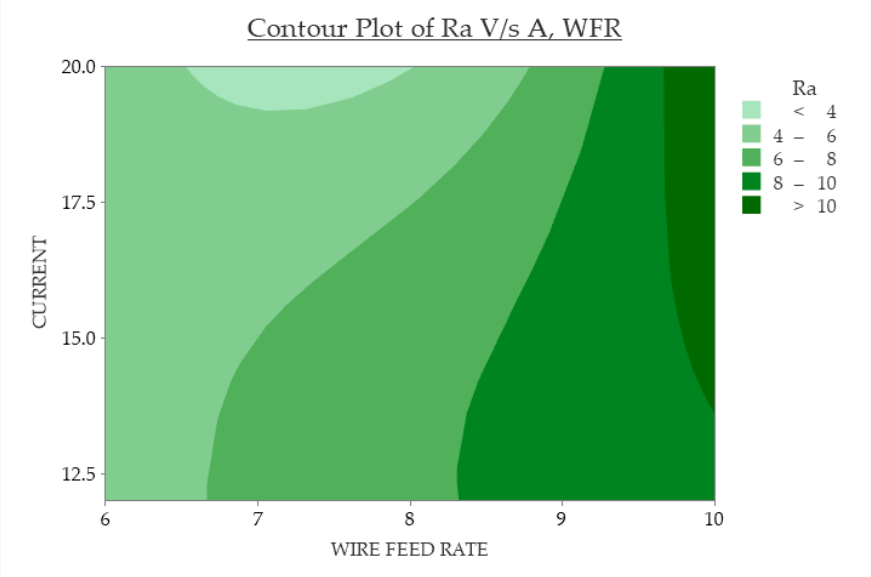

Figure 10 Contour surface plot: Surface roughness with wire feed& Current rate

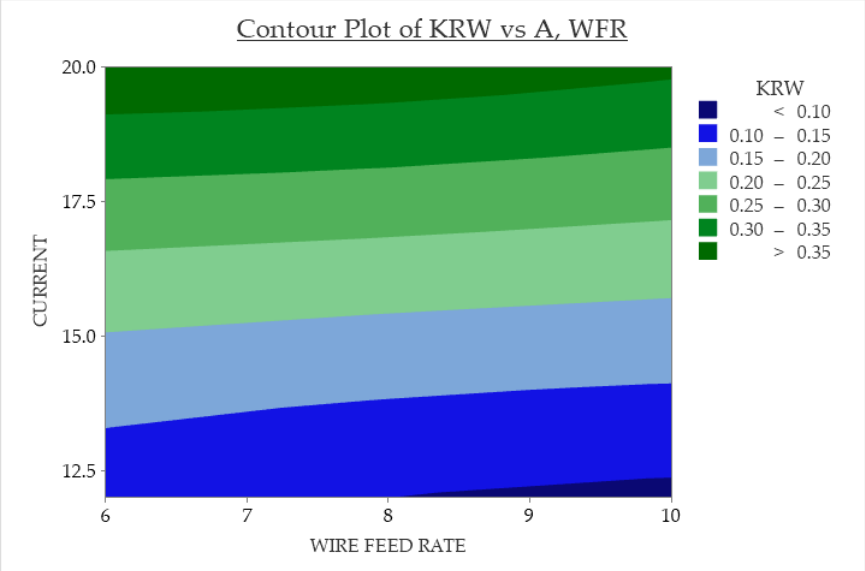

Figure 11 Contour surface plot: Kerf width with Current & rate of feed of wire

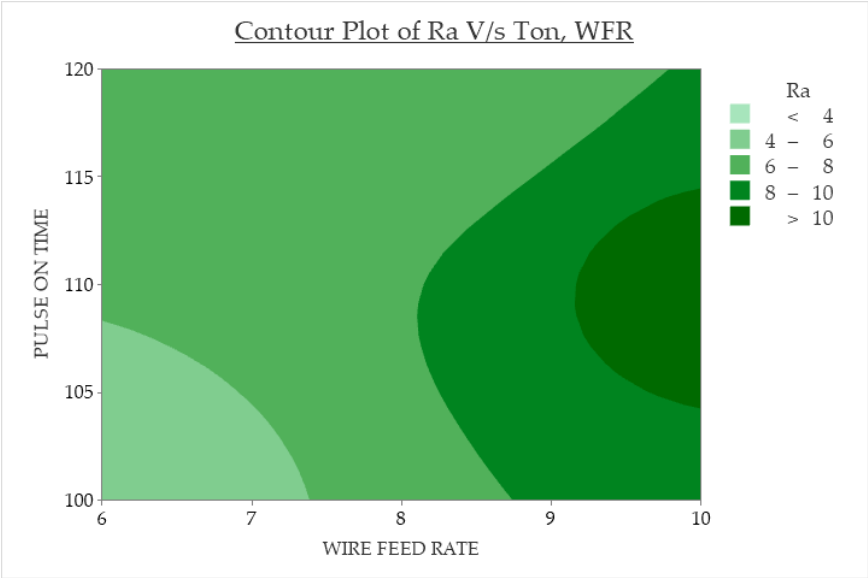

Figure 12 Contour surface plot: Surface roughness with pulse duration& rate of feed of wire

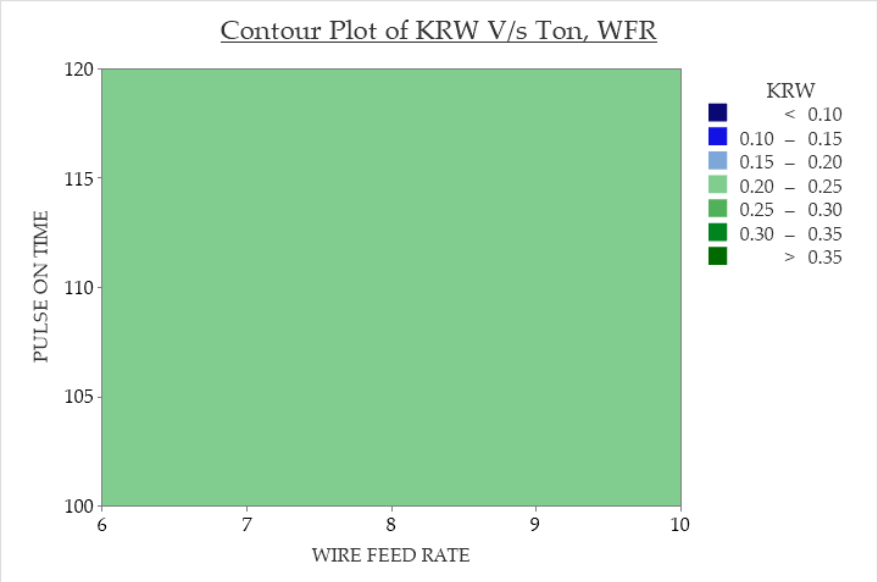

Figure 13 Contour surface plot: Kerf width with pulse duration & rate of feed of wire

5. Conclusions

In this study, it has been investigated that the process variables affect the roughness of WEDM machining. Additionally, it is shown that the best performance characteristics of the machined products made using the WEDM method are produced by the optimal set of processing settings. It is identified that

- The best results of low KRW and R_a are obtained at the 13th experiment and the input data of the 13th experiment are 12A current, 8m/min rate of feed of wire and pulse duration of 100µs.
- The test results show that a decrease in surface roughness is identified with higher current and a decrease in kerf width, due to lower current. But a higher current reduces the material removal area by improving the R_a.
- Lower pulse-on-time is preferred for improved surface roughness and a medium level pulse-on-time improves the kerf width. The increased pulse-on-time leads to an increased material removal by diminishing the surface finish.
- The higher rate of feed of wire reduces the kerf width, but increases the surface roughness,

which prefers a lower wire feed. The quality of dielectric medium is found satisfactory and it is successfully monitored using the IoT.

6. References

Akhtar, M., & Khajuria, A. (2023). The Synergistic effects of Boron and Impression Creep Testing during Paced Controlling of Temperature for P91 Steels. *Advanced Engineering Materials*, *25*(16), Article 2300053. https://doi.org/10.1002/adem.202300053

Badizi, R. M., Parizad, A., Askari-Paykani, M., & Shahverdi, H. R. (2020). Optimization of mechanical properties using D-optimal factorial design of experiment: Electromagnetic stir casting process of A357− SiC nanocomposite. *Transactions of Nonferrous Metals Society of China*, *30*(5), 1183-1194. https://doi.org/10.1016/S1003-6326(20)65288-8

Boutrih, L., Makich, H., Nouari, M., & Ayed, L. B. (2022). Surface quality in dry machining of CFRP composite/Ti6Al4V stack laminate. *Procedia CIRP*, *108*, 758–763. https://doi.org/10.1016/j.procir.2022.03.117

Calam, T. T., & Çakıcı, G. T. (2022). Optimization of square wave voltammetry parameters by response surface methodology for the determination of Sunset yellow using an electrochemical sensor based on Purpald®. *Food Chemistry*, *404*(a), Article 134412. https://doi.org/10.1016/j.foodchem.2022.134412

Cui, G., Meng, Lingzhao, & Zhai, X. (2022). Buckling behaviors of aluminum foam-filled aluminum alloy composite columns under axial compression. *Thin-Walled Structures*, *177*, Article 109399. https://doi.org/10.1016/j.tws.2022.109399

Dhadda, G., Hamed, M., & Koshy, P. (2021). Electrical discharge surface texturing for enhanced pool boiling heat transfer. *Journal of Materials Processing Technology*, *293*, Article 117083. https://doi.org/10.1016/j.jmatprotec.2021.117083

Erol, M., Kısasöz, A., Yaman, P., Karabeyoğlu, S. S., & Barut, U. (2022). A study on high temperature dry sliding wear of AA7050-T4 and effects of the test temperature on microstructure, corrosion behavior, hardness and electrical conductivity. *Materials Today Communications*, *31*, Article 103410. https://doi.org/10.1016/j.mtcomm.2022.103410

Gautam, N., Goyal, A., Sharma, S. S., Oza, A. D., & Kumar, R. (2022). Study of various optimization techniques for electric discharge machining and electrochemical machining processes. *Materials Today: Proceedings*, *57*, 615–621. https://doi.org/10.1016/j.matpr.2022.02.005

Golshan, A., Ghodsiyeh, D., Gohari, S., Ayob, A., & Baharudin, B. H. T. (2013). Optimization of machining parameters during drilling of 7075 aluminium alloy. *Applied Mechanics and Materials*, *248*, 20-25. https://doi.org/10.4028/www.scientific.net/AMM.248.20

Golshan, A., Gohari, S., & Ayob, A. (2012). Multi-objective optimisation of electrical discharge machining of metal matrix composite Al/SiC using non-dominated sorting genetic algorithm. *International Journal of Mechatronics and Manufacturing Systems*, *5*(5/6), 385–398. https://doi.org/10.1504/IJMMS.2012.049972

Govindarajulu, J. (2021). Comparative regression and neural network modeling of roughness and kerf width in CO_2 laser cutting of aluminium. *Tehničkivjesnik*, *28*(5), 1437–1441. https://doi.org/10.17559/TV-20190130153849

Gu, W., Kunieda, M., & Zhao, W. (2023). Measurement of discharge reaction force under different discharge conditions in WEDM using Hopkinson bar method. *Precision Engineering*, *79*, 52-59. https://doi.org/10.1016/j.precisioneng.2022.09.001

Hynes, N. R. J., Sankaranarayanan, R., Sujana, J. A. J., Krolczyk, G. M., & Ene, A. (2022). Decision tree approach based green flow-drilling of hybrid aluminium matrix composites using eco-friendly coolants. *Journal of Manufacturing Processes*, *80*, 178-186. https://doi.org/10.1016/j.jmapro.2022.05.050

Jithin, S., & Joshi, S. S. (2021) Surface topography generation and simulation in electrical discharge texturing: A review. *Journal of Materials Processing Technology*, *298*,

Article 117297. https://doi.org/10.1016/j.jmatprotec.2021.117297

Joshi, S., Govindan, P., Malshe, A., & Rajurkar, K. (2011). Experimental characterization of dry EDM performed in a pulsating magnetic field. *CIRP Annals*, *60*(1), 239–242. https://doi.org/10.1016/j.cirp.2011.03.114

Khajuria, A., Akhtar, M., Pandey, M. K., Singh, M. P., Raina, A., Bedi, R., & Singh, B. (2019). Influence of ceramic Al_2O_3 particulates on performance measures and surface characteristics during sinker EDM of stir cast AMMCs. *World Journal of Engineering*, *16*(4), 526-538. https://doi.org/10.1108/WJE-01-2019-0015

Khajuria, A., Bedi, R. Singh, B. and Akhtar, M. (2018). EDM machinability and parametric optimisation of 2014Al/Al_2O_3 composite by RSM. *International Journal of Machining and Machinability of Materials*, *20*(6), 536–555. https://doi.org/10.1504/IJMMM.2018.096380

Khazaal, S. M., Nimer, N. S., Szabolcs, S., & Abdulsamad, H. J. (2022). Study of manufacturing and material properties of the hybrid composites with metal matrix as tool materials. *Results in Engineering*, *16*, Article 100647. https://doi.org/10.1016/j.rineng.2022.100647

Kumar, R., Katyal, P., & Mandhania, S. (2022). Grey relational analysis based multiresponse optimization for WEDM of ZE41A magnesium alloy. *International Journal of Lightweight Materials and Manufacture*, *5*(4), 543–554. https://doi.org/10.1016/j.ijlmm.2022.06.003

Liang, Z. L., Yun, T. J., Oh, W. B., Lee, B. R., & Kim, I. S. (2020). A study on MOORA-based Taguchi method for optimization in automated GMA welding process. *Materials Today: Proceedings*, *22*, 1778–1785. https://doi.org/10.1016/j.matpr.2020.03.011

Paulson, D. M., Saif, M., & Zishan, M. (2022). Optimization of wire-EDM process of titanium alloy-Grade 5 using Taguchi's method and grey relational analysis. *Materials Today Proceedings*, *72*, 144-153. https://doi.org/10.1016/j.matpr.2022.06.376

Peta, K., Bartkowiak, T., Galek, P., & Mendak, M. (2021a). Contact angle analysis of surface topographies created by electric discharge machining. *Tribology International*, *163*, Article 107139. https://doi.org/10.1016/j.triboint.2021.107139

Peta, K., Mendak, M., & Bartkowiak, T. (2021b). Discharge energy as a key contributing factor determining microgeometry of aluminum samples created by electrical discharge machining. *Crystals*, *11*(11), Article 1371. https://doi.org/10.3390/cryst11111371

Roy, N. G., Mondal, D., Dey, P., & Ghosh, M. (2022). Optimization of electrical process parameters of WEDM on ECAP Al7075 alloys considering Radial Overcut (ROC) as output response. *Materials Today Proceedings*, *62*(10), 6004-6008. https://doi.org/10.1016/j.matpr.2022.04.982

Saravanan, M., Ramalingam, D., Manikandan, G., & Kaarthikeyen, R. R. (2012). Multi objective optimisation of drilling parameters using Genetic Algorithm. *Procedia Engineering*, *38*, 197–207. https://doi.org/10.1016/j.proeng.2012.06.027

Singh, H., Singh, K., Vardhan, S., & Mohan, S. (2022). A comprehensive review on the new developments consideration in a stir casting processing of aluminum matrix composites. *Materials Today: Proceedings*, *60*(2), 974-981. https://doi.org/10.1016/j.matpr.2021.12.359

Sudhakar, A. N., Markandeya, R., Srinivasa Rao, B., Pandey, A. K., & Kaushik, D. (2022). Effect of alloying elements on the dry sliding wear behavior of high chromium white cast iron and Ni-hard iron. *Materials Today Proceedings*, *60*(3), 1303–1309. https://doi.org/10.1016/j.matpr.2021.09.295

Tan, Z. Y., Wu, X., Guo, J. W., & Zhu, W. (2022). Toughness mechanism and plastic insensitivity of submicron second phase Ta in a novel Ta–$Hf_6Ta_2O_{17}$ composite ceramic. *Ceramics International*, *49*(2), 1932-1939. https://doi.org/10.1016/j.ceramint.2022.09.158

Tata, N., Pacharu, R. K., & Devarakonda, S. K. (2021). Multi response optimization of process parameters in wire-cut EDM on INCONEL 625. *Materials Today: Proceedings*, *47*(19), 6960–6964. https://doi.org/10.1016/j.matpr.2021.05.214

Velavan, K., Palanikumar, K., Dhanush, V., Rajapandiyan, S., Kumar, U. T., &

Aishwarya, M. (2023). Corrosion and microstructure studies on magnesium alloy composite reinforced with mSiCp fabricated via powder metallurgy. *Materials Today: Proceedings*, *72*, 2132–2138. https://doi.org/10.1016/j.matpr.2022.08.235

Wang, X., Yao, P., Li, Y., Zhou, H., Xiao, Y., Deng, M., ... & Zhou, P. (2023). Effects of material transfer evolution on tribological behavior in CuCrZr alloy paired with 7075 al alloy under current-carrying. *Tribology International*, *179*, Article 107960. https://doi.org/10.1016/j.triboint.2022.107960

Xie, J., Sun, P., & Yang, D. (2021). Adaptive fuzzy-based composite anti-disturbance control for a class of switched nonlinear systems with unknown backlash-like hysteresis. *Journal of the Franklin Institute*, *358*(10), 5213–5236. https://doi.org/10.1016/j.jfranklin.2021.04.041

Yan, W., Meng, X., Cui, X., Liu, Y., Chen, Q., & Jin, L. (2022). Evaporative cooling performance prediction and multi-objective optimization for hollow fiber membrane module using response surface methodology. *Applied Energy*, *325*, Article 119855. https://doi.org/10.1016/j.apenergy.2022.119855

Zhang, L., Wang, W., Zhou, N., Dong, X., Yuan, F., & Rujie, H. (2022a or b). *Low temperature fabrication of Cf/BNi/*($Ti_{0.2}Zr_{0.2}Hf_{0.2}Nb_{0.2}Ta_{0.2}$) C-SiCm high entropy ceramic matrix composite by slurry coating and laminating combined with precursor infiltration and pyrolysis." *Journal of the European Ceramic Society*, *42*(7), 3099–3106. https://doi.org/10.1016/j.jeurceramsoc.2022.02.021

Zhu, M., Wang, J., Yang, X., Zhang, Y., Zhang, L., Ren, H., ... & Ye, L. (2022). A review of the application of machine learning in water quality evaluation. *Eco-Environment and Health*, *1*(2), 107–116. https://doi.org/10.1016/j.eehl.2022.06.001